Published in final edited form as:
Biochemistry. 2012 October 2; 51(39): 7654–7664. doi:10.1021/bi3007115.

Hydrophobic Contributions to the Membrane Docking of Synaptotagmin 7 C2A Domain: Mechanistic Contrast Between Isoforms 1 and 7

Devin S. Brandt[†,‡,§,χ], **Matthew D. Coffman**[‡,χ], **Joseph J. Falke**[‡], and **Jefferson D. Knight**[†,‡,*]

[†]Molecular Biophysics Program and Department of Chemistry and Biochemistry, University of Colorado, Campus Box 596, Boulder, CO 80309

[‡]Department of Chemistry, University of Colorado Denver, Campus Box 194, P.O. Box 173364, Denver, CO 80217

Abstract

Synaptotagmin (Syt) triggers Ca^{2+}-dependent membrane fusion via its tandem C2 domains, C2A and C2B. The seventeen known human isoforms are active in different secretory cell types, including neurons (Syt1 and others) and pancreatic β cells (Syt7 and others). Here, quantitative fluorescence measurements reveal notable differences in the membrane docking mechanisms of Syt1 C2A and Syt7 C2A to vesicles comprised of physiological lipid mixtures. In agreement with previous studies, the Ca^{2+} sensitivity of membrane binding is much higher for Syt7 C2A. We report here for the first time that this increased sensitivity is due to the slower target membrane dissociation of Syt7 C2A. Association and dissociation rate constants for Syt7 C2A are found to be ~2-fold and ~60-fold slower than Syt1 C2A, respectively. Furthermore, the membrane dissociation of Syt7 C2A but not Syt1 C2A is slowed by Na_2SO_4 and trehalose, solutes that enhance the hydrophobic effect. Overall, the simplest model consistent with these findings proposes that Syt7 C2A first docks electrostatically to the target membrane surface, then inserts into the bilayer via a slow hydrophobic mechanism. In contrast, the membrane docking of Syt1 C2A is known to be predominantly electrostatic. Thus, these two highly homologous domains exhibit distinct mechanisms of membrane binding correlated with their known differences in function.

C2 domains are central components of many cellular signaling pathways, including secretion, chemotaxis, and cell growth (1-3). Initially identified as homologues of the second conserved domain of protein kinase C (PKC), over 400 of these domains have been identified in human proteins to date (4, 5). One major function of C2 domains is targeting membrane surfaces upon binding one or more Ca^{2+} ions (2, 3, 6). This activity drives Ca^{2+}-sensitive membrane docking of soluble parent proteins (e.g., conventional PKCs), or drives additional membrane docking for proteins already tethered to a membrane [e.g., synaptotagmins (Syt)].

C2 domains are known to dock to their target membranes via various combinations of electrostatic and hydrophobic interactions. For example, the C2 domain from protein kinase

[*]Author to whom correspondence should be addressed jefferson.knight@ucdenver.edu Voice: 303-556-6639 Fax: 303-556-4776 .
[§]Present Address: Department of Chemistry, UCLA, 607 Charles E. Young Drive East Box 951569, Los Angeles, CA 90095-1569
χD.S.B. and M.D.C. contributed equally to this work.

Supporting Information Available: Figures are provided showing lack of C2 domain-membrane FRET in the absence of Ca^{2+} and lack of Syt C2A domain membrane binding induced by sodium sulfate in the absence of Ca^{2+}, as well as three representative movies of single-molecule diffusion. This material is available free of charge via the Internet at http://pubs.acs.org.

Cα (PKCα C2) binds to anionic headgroups of phosphatidylserine (PS) and phosphatidylinositol-(4,5)-bisphosphate [PI(4,5)P_2, PIP_2], while the C2 domain from cytosolic phospholipase A_2 (cPLA_2 C2) penetrates deeply into the hydrocarbon core of phosphatidylcholine (PC)-rich membranes (7-9). This difference in target lipid specificity yields the observed difference in intracellular targeting; PKCα is targeted to plasma membrane while cPLA_2 translocates to internal membranes during a Ca^{2+} signaling event (7, 8, 10, 11). Deeply inserting C2 domains such as cPLA_2 C2 typically exhibit slower membrane association and dissociation rates than domains that interact mainly with headgroups, such as PKCβ C2 or the first C2 domain from synaptotagmin 1 (Syt1 C2A) (9, 12, 13). Among C2 domains that target anionic lipid headgroups, some have been observed to specifically recognize PIP_2 in addition to the more abundant PS (e.g., PKCα C2 and Syt1 C2B) (8, 11, 14, 15), while others appear to use less specific electrostatic interactions (e.g., Syt1 C2A) (16, 17).

Syt family proteins serve as Ca^{2+}-sensitive triggers for membrane fusion in secretory cells (18-20). Seventeen human isoforms are known, each of which contains two C2 domains (C2A and C2B) and an N-terminal transmembrane helix (21-23). Of the known isoforms, Syt1 is by far the most widely studied and is well known to localize to neurosecretory vesicles (19, 21). Syt1 plays a central role in rapid neurotransmitter secretion, and other isoforms including Syt2 and Syt9 are also involved in this process (17, 21).

Other cell types use Syt isoforms for secretion in processes that involve lower peak Ca^{2+} signals and slower response times than neurons. For example, Syt7 is the primary isoform responsible for Ca^{2+}-triggered insulin secretion by the β cells of the pancreas, while Syt1 and Syt2 are not detected in primary β cells (21, 24, 25). The N-terminal helix of Syt7 is anchored predominantly to insulin secretory vesicles in β cells, although it has been observed in other intracellular locations depending on expression level and cell type (24, 26, 27). Syt7 is also found in lysosomal membranes of macrophages, where it is suggested to play a role in their exocytosis (28).

Homologous C2 domains from within the same protein family (e.g., PKC C2 domains, or Syt C2A domains) have been reported to exhibit differences in membrane binding, such as altered Ca^{2+} binding cooperativity and affinity, that tune different isoforms for their distinct functional and cellular contexts (29, 30). C2A domains of Syt isoforms are known to vary in Ca^{2+} sensitivity of membrane binding, with Syt7 C2A being one of the most Ca^{2+}-sensitive (30). Despite known differences in Ca^{2+}-triggered membrane binding *affinity*, C2 domains of the same protein family typically exhibit the same binding *mechanism*.

Here, we report significant differences in the Ca^{2+}-dependent membrane binding reactions of C2A domains from Syt1 and Syt7. In contrast to the rapid membrane association and dissociation rates characteristic of Syt1 C2A, the corresponding domain from Syt7 displays slow kinetics reminiscent of those of cPLA_2 C2 (7, 12). Solute sensitivities of dissociation kinetics are consistent with a significant role of the hydrophobic effect for Syt7 C2A membrane interaction. The simplest interpretation is that membrane-bound Syt7 C2A possesses stronger hydrophobic interactions with the bilayer than Syt1 C2A, although other explanations cannot yet be ruled out. Based on these results, we propose a two-state docking model for Syt7 C2A, wherein the domain initially binds the membrane surface via electrostatic interactions and is subsequently stabilized by hydrophobic insertion.

Materials and Methods

Materials

All lipids were synthetic unless otherwise indicated. Cholesterol (CH), 1-palmitoyl-2-oleoyl-*sn*-glycero-3-phosphocholine (phosphatidylcholine, PC), 1-palmitoyl-2-oleoyl-*sn*-glycero-3-phosphoethanolamine (phosphatidylethanolamine, PE); phosphatidylinositol (PI) natural from bovine liver; 1-palmitoyl-2-oleoyl-*sn*-glycero-3-phosphoserine (phosphatidylserine, PS); 1-palmitoyl-2-oleoyl-*sn*-glycero-3-phospho-(1′-*rac*-glycerol) (phosphatidylglycerol, PG); sphingomyelin (SM) natural from brain; and phosphatidylinositol-4,5-bisphosphate [PI(4,5)P_2, PIP_2] natural from brain were from Avanti. *N*-[5-(dimethylamino)naphthalene-1-sulfonyl]-1,2-dihexadecanoyl-*sn*-glycero-3-phosphoethanolamine (dansyl-PE, dPE) was from Invitrogen. Other chemicals were of high-quality USP or analytical grade.

Cloning, protein expression, and purification

Human Syt7 DNA was obtained from American Type Culture Collection (clone 11045721). The C2A domain (residues N135-S266, based on numbering in GenBank AAI25171) was PCR-amplified and subcloned into a GST expression vector developed previously by the Falke laboratory (31). Fusion protein was expressed in *E. coli* and purified using a glutathione affinity column, including extensive washing with 0.5 M NaCl to remove any nonspecifically bound nucleic acids prior to cleavage with thrombin and elution of the free C2 domain. $cPLA_2$ C2, PKCα C2, and rat Syt1 C2A were also expressed as GST fusions, as described previously, and purified by the same method (7, 12). The $cPLA_2$ C2 domain was further purified by Ca^{2+}-dependent binding to PC-phenyl sepharose resin, followed by elution with ethylenediamine tetraacetic acid (EDTA) (32). Proteins were stored in Buffer A [140 mM KCl, 15 mM NaCl, 25 mM *N*-(2-hydroxyethyl)piperazine-*N*-2-ethanesulfonic acid (HEPES), pH 7.4]. Any residual nucleic acid contamination (assessed by absorbance at 260 nm) was removed by benzonase treatment followed by extensive buffer exchange in a centrifugal concentrator. Protein purity was ≥ 95% as determined by SDS-PAGE, identity was verified using mass spectrometry, and concentration was determined by absorbance at 280 nm in 5M guanidinium HCl.

Preparation of lipid mixtures and phospholipid vesicles

Lipids in chloroform were mixed at the desired molar ratios, dried under a stream of nitrogen, and then further dried under vacuum for 2 hours. The dried lipids were then hydrated with Buffer A. Small unilamellar phospholipid vesicles were generated by sonicating the hydrated lipids to clarity with a Misonix XL2020 probe sonicator. The vesicle stock solutions used in the equilibrium Ca^{2+} titrations and kinetic experiments were prepared with a total accessible lipid concentration of 1.5 mM with the mole percentages for target membranes given in Table 1.

Steady-state fluorescence spectroscopy

Steady-state fluorescence experiments were carried out on a Photon Technology International QM-2000-6SE fluorescence spectrometer at 25 °C. The excitation and emission slit widths were 1 and 8 nm, respectively, for all measurements. All buffers were made with Chelex-treated Ca^{2+}-free water. Protein and vesicle stock solutions were incubated with Chelex resin to remove residual Ca^{2+} before use. Quartz cuvettes and stir bars were decalcified by soaking in 50 mM EDTA and rinsing extensively with Ca^{2+}-free water prior to use.

Equilibrium measurement of Ca^{2+}-dependent protein-to-membrane FRET

To determine the $Ca_{1/2}$ of each C2 domain, protein-membrane binding assays were performed as described previously (33). Briefly, protein (0.5 μM) was added to vesicles (100 μM total accessible lipid) in a quartz cuvette. $CaCl_2$ was titrated in to each cuvette, and fluorescence resonance energy transfer (FRET) was measured with 284 nm excitation, 512 nm emission, and 10 s integration. Each intensity value was corrected for dilution, and the intensity of a blank sample was subtracted containing only buffer, lipid, and Ca^{2+}. Reversibility was verified following all Ca^{2+} titrations by measuring fluorescence after addition of sufficient EDTA to chelate all free calcium. Data were fit using *Kaleidagraph* (Synergy Software) to the Hill equation,

$$\Delta F = \Delta F_{max} \frac{\left[Ca^{2+}\right]^H}{\left[Ca^{2+}\right]^H + (Ca_{1/2})^H} \quad (1)$$

where ΔF is the fluorescence increase, H is the Hill coefficient, and ΔF_{max} is the calculated maximal fluorescence change. Data in figures are shown following normalization of ΔF_{max} to unity for each titration, except where noted otherwise.

Equilibrium fluorescence measurements were performed in Buffer A. For a subset of Ca^{2+} titrations, including those for which $Ca_{1/2} < 3$ μM, a Ca^{2+} buffering system including 1.5 mM nitrilotriacetic acid (NTA) and 1 mM $MgCl_2$ was used in order to maintain total Ca^{2+} well in excess of protein. In these titrations, the free Ca^{2+} concentration was calculated using MaxChelator (http://www.stanford.edu/~cpatton/webmaxcS.htm). Reliability of this system is demonstrated by measurements with Syt7 C2A on TM(−)PIP_2 both in the presence and absence of this Ca^{2+} buffering system, whose $Ca_{1/2}$ values differ by < 20% (Table 2).

Equilibrium measurement of ionic strength dependence of membrane binding

C2 domains (0.5 μM) were premixed with TM(−)PIP_2 vesicles (100 μM total accessible lipid) in Buffer A + 1 mM $MgCl_2$ and excess $CaCl_2$. The Ca^{2+} concentrations used were 1 mM for Syt1 C2A and 200 μM for Syt7 C2A, since liposome flocculation was sometimes observed with Syt7 C2A at higher Ca^{2+} concentrations. These Ca^{2+} concentrations are well in excess of $Ca_{1/2}$, resulting in a maximal FRET efficiency as monitored by dansyl emission at 512 nm. NaCl was titrated into each cuvette and fluorescence was measured as described above, with a sample lacking protein serving as a blank. A baseline value of fluorescence due to direct dansyl excitation at 284 nm was obtained by adding sufficient EDTA to fully chelate calcium at the end of the titration. This value was subtracted from all measurements, and the corrected initial fluorescence intensity was normalized to unity.

Stopped-flow measurement of association and dissociation kinetics

All kinetic experiments were performed on an Applied Photophysics SX.17 stopped -flow fluorescence spectrophotometer at 25 °C in Buffer A, unless otherwise indicated. The dead time of the instrument was 0.9 ± 0.1 ms; thus, all data points prior to 1 ms were eliminated prior to quantitative analysis. The excitation wavelength and slit-width settings on the excitation monochromator were 284 and 6 nm, respectively, and a 475-nm longpass filter was used for detecting dansyl (acceptor) emission. To determine the observed rate constant for membrane association (k_{obs}), C2 domains (0.5 μM, all concentrations after mixing) and Ca^{2+} (200 μM) were rapidly mixed with vesicles (100 μM total accessible lipid). The resulting time course exhibited increasing fluorescence intensity with time, which was fit to a single exponential function:

$$F = \Delta F_{\max}\left(1 - e^{-k_{obs}t}\right) + C \quad (2)$$

where k_{obs} is the apparent association rate constant and C is an offset. To simplify representations, C was subtracted and $\Delta F_{\max}$ normalized to unity in figures shown.

To determine the rate constant for the dissociation (k_{off}) of C2 domains from the membranes, the ternary complex of C2 domains (0.5 μM), vesicles (100 μM total accessible lipid), and Ca^{2+} (200 μM) was assembled. The ternary complex was then rapidly mixed with an equal volume of EDTA (1 mM after mixing). The return to equilibrium was monitored using the decrease in protein-to-membrane FRET judged by dansyl emission as the C2 domain dissociated from the membrane. The data were subjected to nonlinear least-squares fitting to a single- or double-exponential function (Eq 3 or 4, respectively):

$$F = \Delta F_{\max}\left(e^{-k_{off}t}\right) + C \quad (3)$$

$$F = \Delta F_{\max 1}\left(e^{-k_{off1}t}\right) + \Delta F_{\max 2}\left(e^{-k_{off2}t}\right) + C \quad (4)$$

where the k_{off} are dissociation rate constants and C is an offset. Similarly to association plots, C was subtracted and $\Delta F_{\max}$ (or $\Delta F_{\max 1} + \Delta F_{\max 2}$) normalized to unity in figures shown.

Single-molecule diffusion measurement

Protein lateral diffusion was measured using total internal reflection fluorescence (TIRF) microscopy essentially as described previously (34, 35). C2 domains were engineered to include the 11-amino acid recognition sequence for Sfp phosphopantetheinyltransferase and labeled using this enzyme (34, 36). Supported lipid bilayers containing a 3:1 mixture of DOPC and DOPS were prepared as described previously (34). These were imaged in single-molecule imaging buffer (Buffer A with 20 mM 2-mercaptoethanol, 0.5 mM $MgCl_2$, and 200 μM $CaCl_2$) at 20 °C before and after addition of protein. Images were taken on a TIRF microscope with simultaneous excitation at 532 and 640 nm, and the two emission wavelengths were imaged simultaneously from the same view area on different areas of the CCD camera. Particles were tracked using ImageJ and diffusion constants were determined in *Mathematica* (Wolfram Research) as described previously (34).

Results

Strategy

The goal of this study is to compare the kinetic and equilibrium membrane binding properties of Syt7 C2A to those of the well-studied Syt1 C2A, in order to shed light on the mechanism underlying the known, higher Ca^{2+}-sensitivity of Syt7 C2A that is crucial for its signaling function. The domains were expressed in *E. coli* as GST fusions, purified by affinity chromatography, and eluted following thrombin cleavage between the GST and C2 domains. In addition, $cPLA_2$ C2 and PKCα C2 domains were isolated as previously described for use in control experiments (7).

In order to best approximate the complexity and negative charge density of the native membranes targeted by these protein domains *in vivo*, except where noted otherwise experiments comparing the two domains were performed with lipid compositions reflecting the content of physiological target membranes (TM, see Methods). It is currently debated whether Syt C2A domains target the plasma membrane or secretory vesicle membrane

during fusion (37-39). Furthermore, the lipid compositions of these two subcellular membranes in β cells have not been reported. However, based on measurements of neuronal secretory vesicle and erythrocyte plasma membrane compositions (40, 41), and assuming similar asymmetry due to flippase activity (42), we estimate that the cytosolic faces of these two membranes have similar lipid compositions approximated by the TM membranes used in this study. One notable exception is the polyanionic lipid $PI(4,5)P_2$, which is found exclusively in the plasma membrane (43, 44). Thus, our experiments compare C2A binding to membranes both lacking $PI(4,5)P_2$ [TM(−)PIP_2] and containing 1% $PI(4,5)P_2$ [TM(+)PIP_2].

Ca^{2+} dependence of C2A-membrane docking

Syt7 C2A has been previously reported to be among the most Ca^{2+}-sensitive Syt C2A domains for docking to simple membranes comprised of PC and PS (30). As a functional test of purified protein, the Ca^{2+} sensitivity of membrane binding was measured using a protein-to-membrane FRET assay previously used in our laboratory with Syt1 C2A (12, 33). Ca^{2+} was titrated into samples containing 0.5 μM Syt1 C2A or Syt7 C2A domain and excess liposomes (SUVs) containing PC:PS (1:1) with 5% dansyl-PE, and the tryptophan-to-dansyl FRET efficiency was measured as a function of [Ca^{2+}] (Figure 1). Fitting of titration curves to the Hill equation yielded Hill cooperativity coefficients and $Ca_{1/2}$ values, defined as the concentration of Ca^{2+} at which membrane binding is half maximal. The measured $Ca_{1/2}$ values were 31 ± 2 μM and 1.7 ± 0.2 μM for Syt1 C2A and Syt7 C2A, respectively (Figure 1, Table 2). Hill coefficients for both domains were greater than 1, as expected for cooperative binding of multiple Ca^{2+} ions by each domain (9, 14, 32). The $Ca_{1/2}$ value of Syt1 C2A is similar to that reported previously in our laboratory using the same lipid composition (12), and the $Ca_{1/2}$ value of Syt7 C2A is comparable with a previous report using 3:1 PC:PS and GST-fused protein (30).

Syt1 C2A is known to target anionic lipids nonspecifically, with no significant preference for $PI(4,5)P_2$ (16). Syt7 C2A has been reported to bind PC/1.5%$PI(4,5)P_2$ membranes in a Ca^{2+}-dependent manner, but the effect of $PI(4,5)P_2$ on its Ca^{2+} sensitivity toward PS-containing membranes has not been tested (45). Here, Ca^{2+} titrations were carried out to measure Syt1 C2A and Syt7 C2A docking to physiological target membranes with and without $PI(4,5)P_2$ [TM(+)PIP_2 and TM(−)PIP_2], and the fit parameters are reported in Table 2. $Ca_{1/2}$ values on TM(−)PIP_2 were slightly greater than those on PC:PS (1:1) membranes for both domains, as expected due to the lower density of anionic lipids in TM(−)PIP_2. Addition of $PI(4,5)P_2$ to generate the TM(+)PIP_2 mixture decreased $Ca_{1/2}$ values by less than 30% for both C2A domains. This behavior is clearly distinct from that reported for PKCα C2, whose $Ca_{1/2}$ is strongly dependent on the presence of $PI(4,5)P_2$ (7, 8, 46). As a positive control, a 4-fold $Ca_{1/2}$ decrease was measured in parallel studies of PKCα C2 binding to the same TM(+)PIP_2 and TM(−)PIP_2 membranes (Table 2). In other control measurements, FRET was not observed for either C2A domain in the presence of membranes containing only PC and dPE (Figure 1), nor with PS-containing membranes in the absence of Ca^{2+} (Supporting Material, Figure S1). Overall, these observations are consistent with both domains having a Ca^{2+}-dependent association with anionic lipids but without significant enhancement derived from additional targeting to $PI(4,5)P_2$.

Electrostatic contributions to membrane docking

In order to directly test for electrostatic contributions to Syt7 C2A membrane interaction, Ca^{2+} titrations were performed with this domain on membranes with varying mole fractions of the anionic lipid PS. Overall, the TM(−)PIP_2 mixture contains 31% anionic lipids (21% PS, 5% PI, and 5% dPE). The measured $Ca_{1/2}$ values increase from 2.2 ± 0.1 μM on membranes containing 31% PS to 8 ± 1 μM on membranes containing 11% PS, reflecting a

large effect of anionic lipid content in apparent membrane affinity (Figure 2, Table 2). When the PS and PI in the TM mixture are quantitatively substituted with the anionic lipid phosphatidylglycerol (PG), Syt7 C2A retains Ca^{2+}-dependent membrane binding with a $Ca_{1/2}$ within error of the standard TM composition [Table 2, TM(−)PS/PI(+)PG]. Clearly, the anionic character of the membrane is a key determinant of Syt7 C2A affinity (Figure 1), reflecting an electrostatic component to the membrane docking interaction similar to that previously reported for Syt1 C2A (16).

To test whether the electrostatic component of membrane interaction is required for Ca^{2+}-triggered Syt7 C2A-membrane docking, NaCl was titrated into C2A/Ca^{2+}/liposome mixtures up to a final concentration of 700 mM (Figure 3). As judged by the observed FRET signal at equilibrium, the membrane affinity of Syt1 C2A decreased steadily during the titration, with nearly complete dissociation achieved above 300 mM NaCl. This NaCl dependence of Syt1 C2A membrane binding has been reported previously by our group and others (12, 47). By contrast, Syt7 C2A remained ~80% bound at 600 mM NaCl. This relative insensitivity to NaCl indicates that Syt7 C2A binds much more tightly to membranes than Syt1 C2A at high ionic strength, and suggests that Syt7 C2A either has an extremely strong electrostatic attraction to the membrane or possesses an additional mechanism stabilizing its membrane-docked state.

Kinetics of C2A-membrane association and dissociation

C2 domains that insert deeply into membranes with extensive hydrophobic contact, such as $cPLA_2$ C2, tend to associate and dissociate from membranes more slowly than domains such as Syt1 C2A and PKCα C2 possessing primarily electrostatic docking (12). We compared the membrane association and dissociation kinetics for Syt1 C2A and Syt7 C2A on TM(−)PIP_2 membranes using stopped-flow fluorimetry. Apparent on-rates were determined in the presence of saturating $CaCl_2$ (200 μM), which upon mixing drives full association of the domains with membrane vesicles. Off-rates were measured by rapid addition of EDTA to pre-mixed C2 domains and vesicles. As positive controls, we also measured the association and dissociation kinetics of $cPLA_2$ C2 and PKCα C2 domains on the same membranes. The association and dissociation rates measured for Syt1 C2A, $cPLA_2$ C2 and PKCα C2 were all within 2-fold of those measured previously for the same proteins (7, 12), with minor differences explained by the different lipid composition of the TM(−)PIP_2 membranes.

The membrane association rate of Syt7 C2A is observed to be comparable to the Syt1 C2A and PKCα C2 domains. In the presence of 100 μM total accessible lipid, Syt7 C2A binds TM(−)PIP_2 vesicles with an apparent rate constant (k_{obs}) of 157 ± 2 s^{-1} (Figure 4A, Table 3). This is 2-fold slower than Syt1 C2A (340 ± 10 s^{-1}) and 2-fold faster than PKCα C2 (64 ± 2 s^{-1}), both of which interact primarily with the headgroup region of membranes. All three of these domains had association curves that fit well to single-exponential equations. The association rate of Syt7 C2A was over 4-fold faster than that of $cPLA_2$ C2 (37 ± 2 s^{-1}, Figure 4A, Table 3). Similarly, the headgroup-binding Syt1 C2A and PKCα C2 domains associated 9-fold and 2-fold faster than $cPLA_2$ C2.

In contrast, the membrane dissociation rate of Syt7 C2A is vastly different from Syt1 C2A and PKCα C2, but is more similar to that of the deeply inserted $cPLA_2$ C2. The dissociation timecourse of Syt7 C2A following EDTA addition fits well to a single-exponential curve with a rate constant k_{off} = 11 ± 4 s^{-1} (Figure 4B, Table 3). By contrast, Syt1 C2A requires a double exponential fit with the major component exhibiting the off-rate constant 670 ± 20 s^{-1}. The minor component was faster than the upper limit of measurement and may be a mixing artifact on this short timescale, as first-order dissociation has been reported previously for this domain (12). $cPLA_2$ C2 dissociation displayed a single exponential rate

constant of 15 ± 1 s^{-1}, in good agreement with a previous report (7). Overall, the dissociation rate of Syt7 C2A is comparable to the deeply penetrating $cPLA_2$ C2 domain and much slower than the headgroup binding domains Syt1 C2A and PKCα C2.

Hydrophobic contributions to membrane docking

The slow dissociation rate of Syt7 C2A is consistent with stabilization from hydrophobic membrane insertion, but could also arise from other factors (see Discussion). In order to test the role of the hydrophobic effect in the slow dissociation of this domain, we measured dissociation kinetics in the presence of a kosmotropic agent, either 30% trehalose or 1.3 M Na_2SO_4. Although their precise mechanism is unknown, these solutes generally increase the free energy penalty for water-exposed nonpolar surfaces (48). Effects include stronger interaction between proteins and nonpolar matrices (e.g., in hydrophobic interaction chromatography), stabilized folded states of proteins, and increased membrane affinity for deeply inserting proteins such as $cPLA_2$ C2 (12, 49-51). The presence of either agent reduced the rate of Syt7 C2A membrane dissociation significantly (Figure 5, Table 3). The effect of Na_2SO_4 is particularly interesting, since the ionic strength of this solution would tend to screen electrostatic interactions and weaken any electrostatic contributions to membrane binding. Indeed, inclusion of 1.3 M NaCl instead of Na_2SO_4 increased the dissociation rate (Figure 5). Inclusion of 30% trehalose decreased the Syt7 C2A dissociation rate ~2-fold but had no significant effect on the dissociation rate of Syt1 C2A (Table 3). The ionic strength sensitivity of Syt1 C2A precluded measurement in 1.3 M Na_2SO_4, since the equilibrium position of this domain in high salt is not on the membrane even in the presence of Ca^{2+} (Figure 3 and data not shown). Na_2SO_4 in the absence of Ca^{2+} was not sufficient to target Syt7 C2A to membranes, in contrast to $cPLA_2$ C2 (Figure S2). Overall, these results indicate that the off rate of Syt7 C2A, but not Syt1 C2A, is sensitive to the inclusion of kosmotropic solutes known to enhance hydrophobic components of biomolecular association.

Lack of self-association of Syt7 C2A

In principle, a hydrophobic contribution to protein-membrane binding could stem from several mechanisms (see Discussion). One possibility of particular interest for Syt7 C2A is protein-protein association, as this domain has been reported to self-associate in solution at high [Ca^{2+}] (52). In order to test for lateral self-association of membrane-bound Syt7 C2A, we measured diffusion on a supported bilayer using single-molecule total internal reflection fluorescence (TIRF) microscopy with particle tracking (Table 4, Movies S1-S3). Alexa Fluor 647-labeled Syt7 C2A (AF647-Syt7C2A, ~5 pM) was used as a probe molecule, and either Alexa Fluor 555-labeled $cPLA_2$ C2 (AF555-$cPLA_2$C2, ~1 pM) or PKCα C2 (AF555-PKCαC2, ~3 pM) was used in the same samples as a negative control. If Syt7 C2A self-associates on the surface, then its diffusion constant should decrease upon addition of unlabeled Syt7 C2A, while diffusion of the control protein should remain constant (34). Instead, addition of 20 nM Syt7 C2A did not change diffusion within measurement error, while 60 nM unlabeled Syt7 C2A decreased diffusion of all species by approximately the same amount (Table 4). The latter effect likely represents crowding on the membrane surface at high protein-to-lipid ratios. Based on the initial spot density of ~5 pM AF647-Syt7C2A, we estimate a ~1:300 protein-to-lipid ratio on the membrane after addition of 20 nM Syt7 C2A, comparable to the maximum 1:200 ratio reached in our ensemble fluorescence experiments. [We note that the cationic Syt7 C2A tends to associate strongly with contaminants from cell lysates similarly to Syt1 C2B (53). The presence of these contaminants (likely nucleic acid, based on absorbance at 260 nm) gave rise to apparent self-association in some of our early experiments (data not shown), but self-association was not observed after the contaminants were removed.] Overall, these data indicate no Syt7 C2A

oligomerization on the bilayer at the protein-to-lipid ratios used for the present equilibrium and kinetic measurements.

Discussion

The membrane targeting mechanism of the Syt1 C2A domain has been the subject of many detailed investigations. The Syt7 C2A domain is less well characterized; it is known to exhibit a higher Ca^{2+} sensitivity than Syt1 C2A, but the molecular mechanisms underlying its higher Ca^{2+} sensitivity and its membrane docking reaction remain unknown. Here we report the following six new observations for Syt7 C2A docking to target membranes composed of a near-physiological lipid mixture. (i) Other anionic lipids, particularly PG, can substitute for PS equally well as a target lipid, indicating that the membrane docking mechanism includes an electrostatic component. (ii) The presence of $PI(4,5)P_2$ causes no enhancement of membrane affinity beyond that expected from nonspecific electrostatic interaction, indicating that $PI(4,5)P_2$ is not a target lipid as observed previously for Syt1 C2A (16). (iii) The Syt7 C2A-membrane interaction is stable in the presence of up to 600 mM NaCl, suggesting that the membrane docking mechanism includes an important non-electrostatic component, in contrast to Syt1 C2A which is displaced from membrane by similar levels of salt (12, 47). (iv) The lateral bilayer diffusion of Syt7 C2A is independent of protein concentration over a broad range of membrane surface densities, indicating that the additional membrane binding stability does not arise from surface-induced oligomerization. (v) The first direct measurement of Syt7 C2A membrane dissociation kinetics indicates they are 60-fold slower than Syt1 C2A dissociation kinetics, and instead are similar to the deeply penetrating $cPLA_2$ C2. Unusually slow dissociation kinetics have also been reported previously for the entire cytoplasmic domain of Syt7 (54), and our current findings provide strong evidence that the C2A domain contributes to or dominates this behavior. (vi) The Syt7 C2A dissociation kinetics are further slowed by kosmotropic solutes, providing evidence that the rate-limiting step in dissociation may involve exposure of hydrophobic residues to solvent.

The $Ca_{1/2}$ values for Syt7 C2A binding to physiological target membranes in this study are within the range reported in previous studies using less quantitative assays with simpler lipid compositions [1-6 μM, (30, 55)]. For comparison, recent studies reported slightly lower $Ca_{1/2}$ values of ≤1 μM for membrane binding of the entire cytoplasmic region and for vesicle fusion induced by full-length Syt7 (56, 57). Thus, while the isolated C2A domain exhibits high Ca^{2+} sensitivity, it appears likely that C2B and/or interdomain interactions play additional roles in the function of full-length Syt7, analogous to recently reported interdomain cooperativity in Syt1 (17, 58-60).

The simplest Syt7 C2A membrane docking mechanism consistent with these observations is the two-step reaction illustrated in Figure 6A. In this model, the domain initially docks to target membrane via nonspecific electrostatic attraction between the positively charged Ca^{2+}-C2 complex and anionic membrane lipids, similar to the electrostatic docking mechanism of many C2 domains including Syt1 C2A (Figure 6A, step 1). In this initial step, Ca^{2+} binding is proposed to serve as an electrostatic switch that changes the protein-membrane electrostatic interaction from unfavorable to favorable (61). Subsequently, the surface-bound Syt7 C2A is proposed to penetrate more deeply into the bilayer, enabling hydrophobic residues to penetrate into the hydrocarbon core (Figure 6A, step 2). Since the protein-to-membrane FRET assay employed here to observe membrane binding detects the initial electrostatic binding step, and the second membrane penetration step is unlikely to significantly alter the FRET signal further, the model adequately explains the observation that Syt7 C2A association kinetics are single-exponential and similar in rate to C2 domains with a purely electrostatic binding mechanism (Figure 4A). During the dissociation reaction,

single exponential kinetics are again observed (Figure 4B), supporting the idea that extraction of the hydrophobic residues from the bilayer is rate-determining and slow relative to the subsequent, rapid dissociation of the electrostatic protein-membrane complex.

Published structures of the two domains offer some possible clues to the structural origin of hydrophobic enhancement for Syt7 C2A. The two C2A domains share 48% identity and 90% conserved polarity in their amino acid sequences (2). Both possess two nonpolar residues that protrude from the ends of two calcium-binding loops; mutation of these in Syt1 C2A influences membrane affinity despite its predominantly electrostatic binding mechanism (Figure 6B,C) (62, 63). For Syt1 C2A these residues are Met173 and Phe234; for Syt7 C2A both hydrophobic residues are Phe (167 and 229). Since aromatic residues including Phe are known to have an unusually high affinity for the region of the bilayer hydrocarbon core adjacent to the headgroup layer, the presence of two Phe residues in Syt7 C2A may account for the stronger hydrophobic contribution to its docking mechanism (64, 65). Figure 6C schematically shows the predicted membrane docking geometry of Syt7 C2A, with both Phe residues penetrating into the hydrocarbon layer, compared to the shallower, experimentally determined docking geometry of Syt1 C2A (Figure 6B) with just one Phe penetrating into this region (13). This proposed geometry of Syt7 C2A somewhat resembles that of Syt1 C2AB; Met173 penetrates into the bilayer more deeply in Syt1 C2AB than in Syt1 C2A (60). Notably, a mutation in *Drosophila* Syt1 corresponding to F234Y diminishes secretion by 50%, suggesting membrane insertion of phenylalanine is a key determinant of protein function (66).

The proposed hydrophobic insertion of Syt7 C2A is supported by its slow dissociation kinetics and the sensitivity of the kinetics to kosmotropic agents that enhance the hydrophobic effect. Both of these features were previously observed for the $cPLA_2$ C2 domain, which has since been shown directly by electron paramagnetic resonance (EPR) membrane docking geometry studies to penetrate into the bilayer hydrocarbon core (9, 12). However, further tests of the Syt7 C2A hydrophobic insertion, including future EPR docking geometry studies, are crucial since the available evidence does not fully rule out alternative models. For example, one could argue that following the electrostatic docking step, a slow conformational change occurs in the Syt7 C2A domain that buries hydrophobic residues inside the protein, rather than in the membrane. Such a conformational change appears less likely than the proposed model, given that no such rearrangement has been observed in other C2 domains, presumably due in part to the highly stable β-sandwich core of the C2 motif. Alternatively, one could argue that the kosmotrope sensitivity of Syt7 C2A dissociation reflects a protein-induced change in membrane structure, for example PS clustering or altered bilayer curvature, since kosmotrope effects on membrane dynamics are unknown. This possibility appears less likely to account for our observation of slow dissociation, since Syt1 C2AB is known to cause such clustering and bending (18, 59) but dissociates rapidly from the membrane upon removal of Ca^{2+} (54).

The slower dissociation kinetics observed for Syt7 C2A directly account for its higher Ca^{2+} sensitivity relative to Syt1 C2A. In principle, the observed higher Ca^{2+} sensitivity for Syt7 C2A relative to Syt1 C2A could arise from either tighter Ca^{2+} binding by the free domain, and/or stronger membrane affinity for the Ca^{2+}-loaded domain. The latter effect has been termed target-assisted messenger affinity (TAMA) (7). Ca^{2+} binding by the two domains in the absence of membrane does not produce a fluorescence change ((12) and data not shown), and thus the intrinsic Ca^{2+} affinity is not accessible via this method. However, the membrane affinity of the Ca^{2+}-loaded domains may be approximated from the ratio of the kinetic parameters k_{off} and k_{on}. Here, k_{on} can be approximated as k_{obs}/[PS] since PS is the major anionic lipid target present in the TM(−)PIP_2 membranes and the protein is essentially 100% bound at equilibrium. Values of k_{off}/k_{on} are shown in Table 3, with Syt7 C2A ~25-

fold lower than Syt1 C2A. This represents a much tighter membrane interaction for Syt7 C2A relative to Syt1 C2A in the presence of 200 μM Ca^{2+}, and could fully account for the 8-fold difference in Ca^{2+} sensitivity measured at equilibrium (Table 2). Such k_{off}/k_{on} values do not correspond directly to equilibrium dissociation constants since membrane docking is accompanied by cooperative binding of multiple Ca^{2+} ions (16, 67). Nevertheless, they show that enhanced membrane affinity of the Ca^{2+} loaded state of Syt7 C2A relative to Syt1 C2A can explain its increased Ca^{2+} sensitivity of membrane binding.

Finally, the observed differences in kinetics and Ca^{2+} sensitivity of membrane binding appear to reflect the physiological roles of the two Syt isoforms. Syt1 is the main isoform involved in rapid neurotransmitter secretion, functioning on a timescale of tens of milliseconds or less (68). Syt7 is more broadly expressed (55) and is responsible for slower secretion of insulin in islet β cells (26) and glucagon in islet α cells (69), as well as lysosomal membrane fusion in macrophages and other cell types (28). Furthermore, neurotransmitter secretion is triggered by peaks of intracellular [Ca^{2+}] in the 100 μM range (70), while insulin secretion is triggered by local [Ca^{2+}] in the 1-10 μM range, comparable to the $Ca_{1/2}$ of Syt7 C2A (71). Thus, dramatically different kinetics and Ca^{2+} sensitivities of the Syt1 and Syt7 C2A domains are well tuned to the timescales and Ca^{2+} levels involved in their cellular functions.

Supplementary Material

Refer to Web version on PubMed Central for supplementary material.

Acknowledgments

We thank Dr. John Corbin for help with Ca^{2+}-free protocols, Dr. Christina Leslie for providing the DNA construct for the $cPLA_2$ C2 domain, Dr. Linda Behlen for assistance with stopped-flow, Dr. Art Pardi for access to the Keck-funded TIRF instrument, the University of Colorado School of Pharmacy mass spectrometry facility for MALDI analysis, and Dr. Scott Reed for critically reading this manuscript.

This work was supported by NIH R01 GM-063235 to J.J.F. and by University of Colorado Denver startup funds to J.D.K.

Abbreviations

PKC	protein kinase C
Syt	synaptotagmin
TM	target membrane
PS	phosphatidylserine
PC	phosphatidylcholine
PI	phosphatidylinositol
PI(4,5)P_2 or PIP_2	phosphatidylinositol-(4,5)-bisphosphate
dPE or dansyl-PE	*N*-[5-(Dimethylamino)napththalene-1-sulfonyl]-1,1-dihexadecanoyl-*sn*-glycero-3-phosphoethanolamine
PG	phosphatidylglycerol
SNARE	soluble N-ethylmaleimide sensitive factor attachment protein receptor
GST	glutathione S-transferase

FRET	fluorescence resonance energy transfer
SUVs	sonicated unilamellar vesicles
EDTA	ethylenediamine tetraacetic acid
NTA	nitrilotriacetic acid
EPR	electron paramagnetic resonance

References

1. Martens S. Role of C2 domain proteins during synaptic vesicle exocytosis. Biochem Soc Trans. 2010; 38:213–216. [PubMed: 20074062]
2. Nalefski EA, Falke JJ. The C2 domain calcium-binding motif: structural and functional diversity. Protein Sci. 1996; 5:2375–2390. [PubMed: 8976547]
3. Cho W, Stahelin RV. Membrane-protein interactions in cell signaling and membrane trafficking. Annu Rev Biophys Biomol Struct. 2005; 34:119–151. [PubMed: 15869386]
4. Coussens L, Parker PJ, Rhee L, Yang-Feng TL, Chen E, Waterfield MD, Francke U, Ullrich A. Multiple, distinct forms of bovine and human protein kinase C suggest diversity in cellular signaling pathways. Science. 1986; 233:859–866. [PubMed: 3755548]
5. Punta M, Coggill PC, Eberhardt RY, Mistry J, Tate J, Boursnell C, Pang N, Forslund K, Ceric G, Clements J, Heger A, Holm L, Sonnhammer EL, Eddy SR, Bateman A, Finn RD. The Pfam protein families database. Nucleic Acids Res. 2012; 40:D290–301. [PubMed: 22127870]
6. Lemmon MA. Membrane recognition by phospholipid-binding domains. Nat Rev Mol Cell Biol. 2008; 9:99–111. [PubMed: 18216767]
7. Corbin JA, Evans JH, Landgraf KE, Falke JJ. Mechanism of specific membrane targeting by C2 domains: Localized pools of target lipids enhance Ca2+ affinity. Biochemistry. 2007; 46:4322–4336. [PubMed: 17367165]
8. Evans JH, Murray D, Leslie CC, Falke JJ. Specific translocation of protein kinase Calpha to the plasma membrane requires both Ca2+ and PIP2 recognition by its C2 domain. Mol Biol Cell. 2006; 17:56–66. [PubMed: 16236797]
9. Malmberg NJ, Van Buskirk DR, Falke JJ. Membrane-docking loops of the cPLA2 C2 domain: detailed structural analysis of the protein-membrane interface via site-directed spin-labeling. Biochemistry. 2003; 42:13227–13240. [PubMed: 14609334]
10. Evans JH, Gerber SH, Murray D, Leslie CC. The calcium binding loops of the cytosolic phospholipase A2 C2 domain specify targeting to Golgi and ER in live cells. Mol Biol Cell. 2004; 15:371–383. [PubMed: 13679516]
11. Stahelin RV, Rafter JD, Das S, Cho W. The molecular basis of differential subcellular localization of C2 domains of protein kinase C-alpha and group IVa cytosolic phospholipase A2. J Biol Chem. 2003; 278:12452–12460. [PubMed: 12531893]
12. Nalefski EA, Wisner MA, Chen JZ, Sprang SR, Fukuda M, Mikoshiba K, Falke JJ. C2 domains from different Ca2+ signaling pathways display functional and mechanistic diversity. Biochemistry. 2001; 40:3089–3100. [PubMed: 11258923]
13. Frazier AA, Roller CR, Havelka JJ, Hinderliter A, Cafiso DS. Membrane-Bound Orientation and Position of the Synaptotagmin I C2A Domain by Site-Directed Spin Labeling. Biochemistry. 2002; 42:96–105. [PubMed: 12515543]
14. Radhakrishnan A, Stein A, Jahn R, Fasshauer D. The Ca2+ affinity of synaptotagmin 1 is markedly increased by a specific interaction of its C2B domain with phosphatidylinositol 4,5-bisphosphate. J Biol Chem. 2009; 284:25749–25760. [PubMed: 19632983]
15. Newton AC, Keranen LM. Phosphatidyl-L-serine is necessary for protein kinase C's high-affinity interaction with diacylglycerol-containing membranes. Biochemistry. 1994; 33:6651–6658. [PubMed: 8204602]
16. Zhang X, Rizo J, Sudhof TC. Mechanism of phospholipid binding by the C2A-domain of synaptotagmin I. Biochemistry. 1998; 37:12395–12403. [PubMed: 9730811]

17. Shin OH, Xu J, Rizo J, Sudhof TC. Differential but convergent functions of Ca2+ binding to synaptotagmin-1 C2 domains mediate neurotransmitter release. Proc Natl Acad Sci U S A. 2009; 106:16469–16474. [PubMed: 19805322]
18. Hui E, Johnson CP, Yao J, Dunning FM, Chapman ER. Synaptotagmin-mediated bending of the target membrane is a critical step in Ca(2+)-regulated fusion. Cell. 2009; 138:709–721. [PubMed: 19703397]
19. Chapman ER. How does synaptotagmin trigger neurotransmitter release? Annu Rev Biochem. 2008; 77:615–641. [PubMed: 18275379]
20. Rizo J, Chen X, Arac D. Unraveling the mechanisms of synaptotagmin and SNARE function in neurotransmitter release. Trends Cell Biol. 2006; 16:339–350. [PubMed: 16698267]
21. Gauthier BR, Wollheim CB. Synaptotagmins bind calcium to release insulin. Am J Physiol Endocrinol Metab. 2008; 295:E1279–1286. [PubMed: 18713958]
22. Craxton M. Synaptotagmin gene content of the sequenced genomes. BMC Genomics. 2004; 5:43. [PubMed: 15238157]
23. Chin H, Choi SH, Jang YS, Cho SM, Kim HS, Lee JH, Jeong SW, Kim IK, Kim GJ, Kwon OJ. Protein kinase A-dependent phosphorylation of B/K protein. Exp Mol Med. 2006; 38:144–152. [PubMed: 16672768]
24. Gao Z, Reavey-Cantwell J, Young RA, Jegier P, Wolf BA. Synaptotagmin III/VII isoforms mediate Ca2+-induced insulin secretion in pancreatic islet beta - cells. J Biol Chem. 2000; 275:36079–36085. [PubMed: 10938083]
25. Grise F, Taib N, Monterrat C, Lagree V, Lang J. Distinct roles of the C2A and the C2B domain of the vesicular Ca2+ sensor synaptotagmin 9 in endocrine beta-cells. Biochem J. 2007; 403:483–492. [PubMed: 17263688]
26. Gauthier BR, Duhamel DL, Iezzi M, Theander S, Saltel F, Fukuda M, Wehrle-Haller B, Wollheim CB. Synaptotagmin VII splice variants alpha, beta, and delta are expressed in pancreatic beta-cells and regulate insulin exocytosis. FASEB J. 2008; 22:194–206. [PubMed: 17709608]
27. Sugita S, Han W, Butz S, Liu X, Fernandez-Chacon R, Lao Y, Sudhof TC. Synaptotagmin VII as a plasma membrane Ca(2+) sensor in exocytosis. Neuron. 2001; 30:459–473. [PubMed: 11395007]
28. Becker SM, Delamarre L, Mellman I, Andrews NW. Differential role of the Ca(2+) sensor synaptotagmin VII in macrophages and dendritic cells. Immunobiology. 2009; 214:495–505. [PubMed: 19157638]
29. Kohout SC, Corbalan-Garcia S, Torrecillas A, Gomez-Fernandez JC, Falke JJ. C2 domains of protein kinase C isoforms alpha, beta, and gamma: activation parameters and calcium stoichiometries of the membrane-bound state. Biochemistry. 2002; 41:11411–11424. [PubMed: 12234184]
30. Sugita S, Shin OH, Han W, Lao Y, Sudhof TC. Synaptotagmins form a hierarchy of exocytotic Ca(2+) sensors with distinct Ca(2+) affinities. Embo J. 2002; 21:270–280. [PubMed: 11823420]
31. Corbin JA, Dirkx RA, Falke JJ. GRP1 pleckstrin homology domain: Activation parameters and novel search mechanism for rare target lipid. Biochemistry. 2004; 43:16161–16173. [PubMed: 15610010]
32. Nalefski EA, Slazas MM, Falke JJ. Ca2+-signaling cycle of a membrane-docking C2 domain. Biochemistry. 1997; 36:12011–12018. [PubMed: 9340010]
33. Nalefski EA, Falke JJ. Use of fluorescence resonance energy transfer to monitor Ca(2+)-triggered membrane docking of C2 domains. Methods Mol Biol. 2002; 172:295–303. [PubMed: 11833355]
34. Knight JD, Lerner MG, Marcano-Velazquez JG, Pastor RW, Falke JJ. Single molecule diffusion of membrane-bound proteins: window into lipid contacts and bilayer dynamics. Biophys J. 2010; 99:2879–2887. [PubMed: 21044585]
35. Ziemba BP, Knight JD, Falke JJ. Assembly of membrane-bound protein complexes: detection and analysis by single molecule diffusion. Biochemistry. 2012; 51:1638–1647. [PubMed: 22263647]
36. Yin J, Straight PD, McLoughlin SM, Zhou Z, Lin AJ, Golan DE, Kelleher NL, Kolter R, Walsh CT. Genetically encoded short peptide tag for versatile protein labeling by Sfp phosphopantetheinyl transferase. Proc Natl Acad Sci U S A. 2005; 102:15815–15820. [PubMed: 16236721]

37. Fuson KL, Montes M, Robert JJ, Sutton RB. Structure of human synaptotagmin 1 C2AB in the absence of Ca2+ reveals a novel domain association. Biochemistry. 2007; 46:13041–13048. [PubMed: 17956130]
38. Vrljic M, Strop P, Ernst JA, Sutton RB, Chu S, Brunger AT. Molecular mechanism of the synaptotagmin-SNARE interaction in Ca2+-triggered vesicle fusion. Nat Struct Mol Biol. 2010; 17:325–331. [PubMed: 20173762]
39. Herrick DZ, Kuo W, Huang H, Schwieters CD, Ellena JF, Cafiso DS. Solution and Membrane-Bound Conformations of the Tandem C2A and C2B Domains of Synaptotagmin 1: Evidence for Bilayer Bridging. Journal of Molecular Biology. 2009; 390:913–923. [PubMed: 19501597]
40. Takamori S, Holt M, Stenius K, Lemke EA, Gronborg M, Riedel D, Urlaub H, Schenck S, Brugger B, Ringler P, Muller SA, Rammner B, Grater F, Hub JS, De Groot BL, Mieskes G, Moriyama Y, Klingauf J, Grubmuller H, Heuser J, Wieland F, Jahn R. Molecular anatomy of a trafficking organelle. Cell. 2006; 127:831–846. [PubMed: 17110340]
41. Voelker, DR. Lipid assembly into cell membranes. In: Vance, DE.; Vance, JE., editors. Biochemistry of Lipids, Lipoproteins and Membranes. 5th Ed. Elsevier; Amsterdam: 2008. p. 441-484.
42. Paterson JK, Renkema K, Burden L, Halleck MS, Schlegel RA, Williamson P, Daleke DL. Lipid specific activation of the murine P4-ATPase Atp8a1 (ATPase II). Biochemistry. 2006; 45:5367–5376. [PubMed: 16618126]
43. van Meer G, Voelker DR, Feigenson GW. Membrane lipids: where they are and how they behave. Nat Rev Mol Cell Biol. 2008; 9:112–124. [PubMed: 18216768]
44. Di Paolo G, De Camilli P. Phosphoinositides in cell regulation and membrane dynamics. Nature. 2006; 443:651–657. [PubMed: 17035995]
45. Tucker WC, Edwardson JM, Bai J, Kim HJ, Martin TF, Chapman ER. Identification of synaptotagmin effectors via acute inhibition of secretion from cracked PC12 cells. J Cell Biol. 2003; 162:199–209. [PubMed: 12860971]
46. Corbalan-Garcia S, Garcia-Garcia J, Rodriguez-Alfaro JA, Gomez-Fernandez JC. A new phosphatidylinositol 4,5-bisphosphate-binding site located in the C2 domain of protein kinase Calpha. J Biol Chem. 2003; 278:4972–4980. [PubMed: 12426311]
47. Hui E, Bai J, Chapman ER. Ca2+-triggered simultaneous membrane penetration of the tandem C2-domains of synaptotagmin I. Biophys J. 2006; 91:1767–1777. [PubMed: 16782782]
48. Creighton, TE. Proteins: structures and molecular properties. 2 ed. Freeman; New York: 1993.
49. Queiroz JA, Tomaz CT, Cabral JM. Hydrophobic interaction chromatography of proteins. J Biotechnol. 2001; 87:143–159. [PubMed: 11278038]
50. Jain NK, Roy I. Effect of trehalose on protein structure. Protein Sci. 2009; 18:24–36. [PubMed: 19177348]
51. Nalefski EA, McDonagh T, Somers W, Seehra J, Falke JJ, Clark JD. Independent folding and ligand specificity of the C2 calcium-dependent lipid binding domain of cytosolic phospholipase A2. J Biol Chem. 1998; 273:1365–1372. [PubMed: 9430670]
52. Fukuda M, Mikoshiba K. Mechanism of the calcium-dependent multimerization of synaptotagmin VII mediated by its first and second C2 domains. J Biol Chem. 2001; 276:27670–27676. [PubMed: 11373279]
53. Ubach J, Lao Y, Fernandez I, Arac D, Sudhof TC, Rizo J. The C2B domain of synaptotagmin I is a Ca2+-binding module. Biochemistry. 2001; 40:5854–5860. [PubMed: 11352720]
54. Hui E, Bai J, Wang P, Sugimori M, Llinas RR, Chapman ER. Three distinct kinetic groupings of the synaptotagmin family: candidate sensors for rapid and delayed exocytosis. Proc Natl Acad Sci U S A. 2005; 102:5210–5214. [PubMed: 15793006]
55. Li C, Ullrich B, Zhang JZ, Anderson RG, Brose N, Sudhof TC. Ca(2+)-dependent and -independent activities of neural and non-neural synaptotagmins. Nature. 1995; 375:594–599. [PubMed: 7791877]
56. Wang P, Chicka MC, Bhalla A, Richards DA, Chapman ER. Synaptotagmin VII is targeted to secretory organelles in PC12 cells, where it functions as a high-affinity calcium sensor. Mol Cell Biol. 2005; 25:8693–8702. [PubMed: 16166648]

57. Zhang Z, Wu Y, Wang Z, Dunning FM, Rehfuss J, Ramanan D, Chapman ER, Jackson MB. Release mode of large and small dense-core vesicles specified by different synaptotagmin isoforms in PC12 cells. Mol Biol Cell. 2011; 22:2324–2336. [PubMed: 21551071]
58. Vrljic M, Strop P, Hill RC, Hansen KC, Chu S, Brunger AT. Post-translational modifications and lipid binding profile of insect cell-expressed full-length mammalian synaptotagmin 1. Biochemistry. 2011; 50:9998–10012. [PubMed: 21928778]
59. Lai AL, Tamm LK, Ellena JF, Cafiso DS. Synaptotagmin 1 modulates lipid acyl chain order in lipid bilayers by demixing phosphatidylserine. J Biol Chem. 2011; 286:25291–25300. [PubMed: 21610074]
60. Herrick DZ, Sterbling S, Rasch KA, Hinderliter A, Cafiso DS. Position of synaptotagmin I at the membrane interface: cooperative interactions of tandem C2 domains. Biochemistry. 2006; 45:9668–9674. [PubMed: 16893168]
61. Murray D, Honig B. Electrostatic control of the membrane targeting of C2 domains. Mol Cell. 2002; 9:145–154. [PubMed: 11804593]
62. Shao X, Fernandez I, Sudhof TC, Rizo J. Solution structures of the Ca2+-free and Ca2+-bound C2A domain of synaptotagmin I: does Ca2+ induce a conformational change? Biochemistry. 1998; 37:16106–16115. [PubMed: 9819203]
63. Gerber SH, Rizo J, Sudhof TC. Role of electrostatic and hydrophobic interactions in Ca(2+)-dependent phospholipid binding by the C(2)A-domain from synaptotagmin I. Diabetes. 2002; 51(Suppl 1):S12–18. [PubMed: 11815451]
64. Wimley WC, White SH. Experimentally determined hydrophobicity scale for proteins at membrane interfaces. Nat Struct Biol. 1996; 3:842–848. [PubMed: 8836100]
65. Hong H, Park S, Jimenez RH, Rinehart D, Tamm LK. Role of aromatic side chains in the folding and thermodynamic stability of integral membrane proteins. J Am Chem Soc. 2007; 129:8320–8327. [PubMed: 17564441]
66. Paddock BE, Wang Z, Biela LM, Chen K, Getzy MD, Striegel A, Richmond JE, Chapman ER, Featherstone DE, Reist NE. Membrane penetration by synaptotagmin is required for coupling calcium binding to vesicle fusion in vivo. J Neurosci. 2011; 31:2248–2257. [PubMed: 21307261]
67. Kertz JA, Almeida PF, Frazier AA, Berg AK, Hinderliter A. The cooperative response of synaptotagmin I C2A. A hypothesis for a Ca2+-driven molecular hammer. Biophys J. 2007; 92:1409–1418. [PubMed: 17114221]
68. Heidelberger R, Heinemann C, Neher E, Matthews G. Calcium dependence of the rate of exocytosis in a synaptic terminal. Nature. 1994; 371:513–515. [PubMed: 7935764]
69. Gustavsson N, Wei SH, Hoang DN, Lao Y, Zhang Q, Radda GK, Rorsman P, Sudhof TC, Han W. Synaptotagmin-7 is a principal Ca2+ sensor for Ca2+ - induced glucagon exocytosis in pancreas. J Physiol. 2009; 587:1169–1178. [PubMed: 19171650]
70. Llinas R, Sugimori M, Silver RB. Microdomains of high calcium concentration in a presynaptic terminal. Science. 1992; 256:677–679. [PubMed: 1350109]
71. Quesada I, Martin F, Soria B. Nutrient modulation of polarized and sustained submembrane Ca2+ microgradients in mouse pancreatic islet cells. J Physiol. 2000; 525(Pt 1):159–167. [PubMed: 10811734]

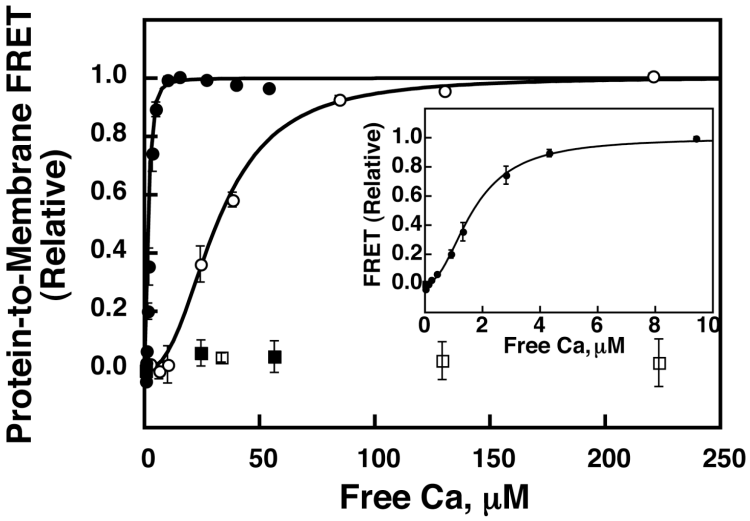

Figure 1. Ca^{2+} sensitivity of membrane binding

$CaCl_2$ was titrated into 0.5 μM Syt1 C2A (open symbols) or Syt7 C2A (closed symbols) in the presence of PC:PS(1:1)/5%dPE or PC/3%dPE vesicles (squares), beginning with Ca^{2+}-free solutions. Protein-to-membrane FRET was measured as described in Methods. Points and error bars shown are mean ± standard deviation of three independent replicate titrations. Data were normalized based on best fits to the Hill Equation (solid curves, Eq. 1); the parameters from these fits are given in Table 2. Data shown are normalized based on these fits. PC control data are normalized to corresponding PC:PS titration data after adjusting for dPE content. Inset shows expansion of the Syt7 C2A binding curve.

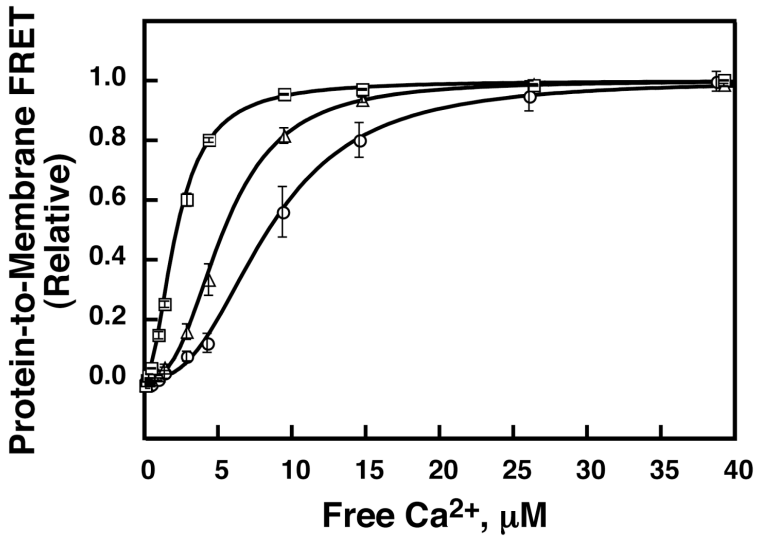

Figure 2. PS sensitivity of Syt7 C2A Ca^{2+}/membrane binding

$CaCl_2$ was titrated into 0.5 μM Syt7 C2A in the presence of membrane vesicles containing different amounts of the anionic lipid PS (squares: TM[31%PS]; triangles: standard TM(−)PIP_2 containing 21% PS; circles: TM[11%PS]). Points and error bars shown are mean ± standard deviation of three independent replicate titrations. Data were normalized based on best fits to the Hill equation (solid curves, Eq. 1); the parameters from these fits are given in Table 2.

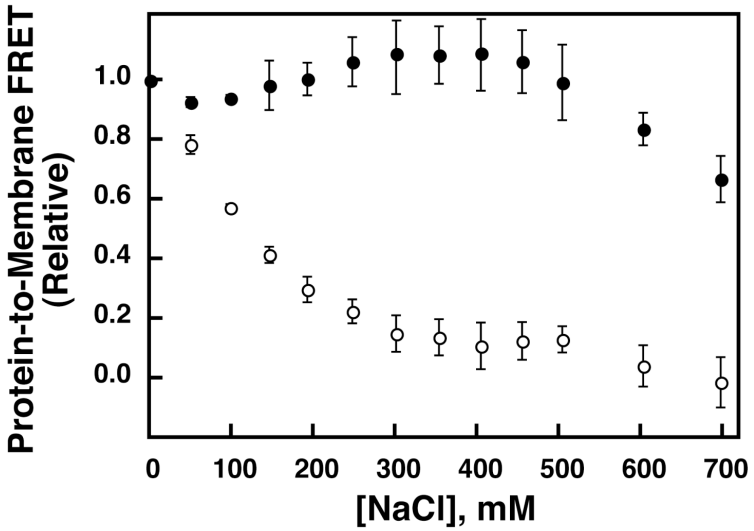

Figure 3. Sensitivity of Syt C2A-membrane interactions to electrostatic screening

Syt1 C2A (0.5 μM, open circles) or Syt7 C2A (0.5 μM, filled circles) was incubated in a fluorescence cell initially in Buffer A containing TM(−)PIP_2 vesicles (100 μM total accessible lipid) and Ca^{2+} at a concentration ~50-fold higher than the $Ca_{1/2}$ (1 mM Ca^{2+} for Syt1 C2A, 200 μM Ca^{2+} for Syt7 C2A). Increasing concentrations of NaCl were added and the protein-to-membrane FRET was measured as described in Methods. Points and error bars shown are mean ± standard deviation of three independent replicate measurements, and are normalized based on the initial fluorescence and the final signal upon addition of EDTA.

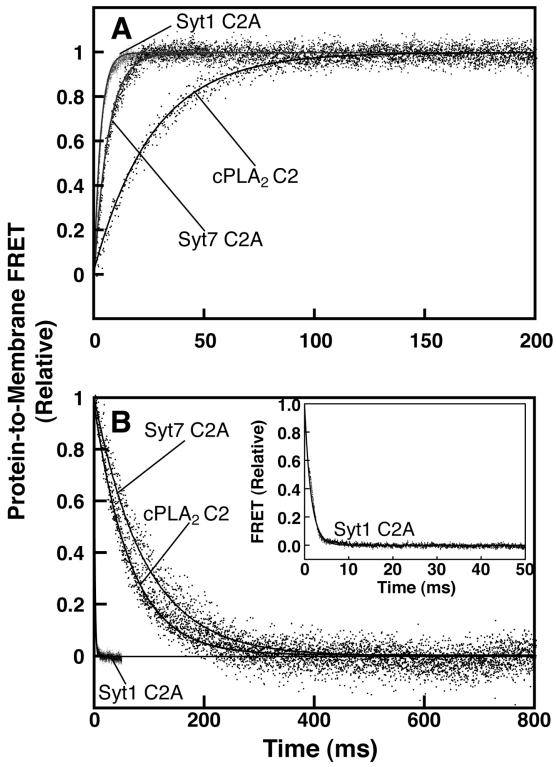

Figure 4. Kinetics of C2 domain-membrane association (A) and dissociation (B)

A: Ca^{2+}-loaded protein (0.5 μM, in buffer A + 200 μM $CaCl_2$) was rapidly mixed with TM(−)PIP_2 vesicles (100 μM accessible lipid; all concentrations are after mixing) in a stopped-flow fluorescence spectrometer, and dansyl fluorescence was monitored as a function of time. Data are normalized based the fits shown to single exponential curves (solid lines, Eq. 2). **B:** Solutions containing 0.5 μM protein, 200 μM $CaCl_2$, and TM(−)PIP_2 vesicles (100 μM accessible lipid) were rapidly mixed with an equal volume of 2 mM EDTA, and protein-to-membrane FRET was observed. Fits shown are to single (Eq. 3, Syt7 C2A and $cPLA_2$ C2) or double (Eq. 4, Syt1 C2A) exponential decays, with rate constants given in Table 3. Inset shows an expansion of the Syt1 C2A timecourse.

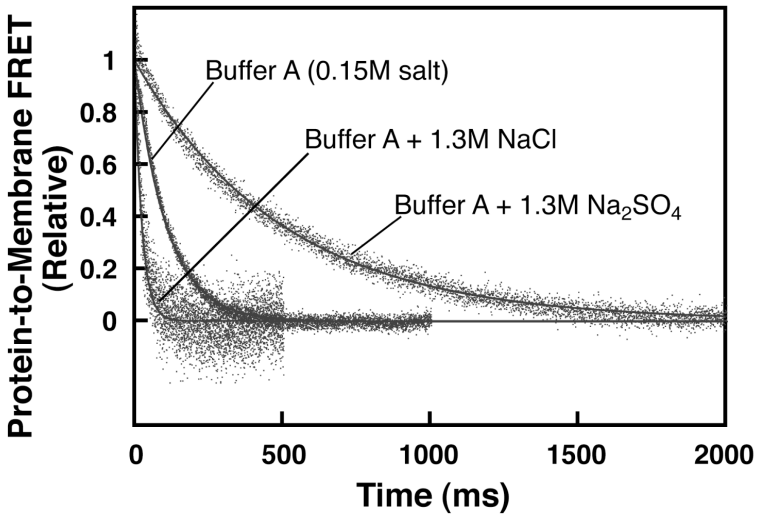

Figure 5. Effect of solutes on Syt7 C2A membrane dissociation

Dissociation was measured as described in the legend to Figure 4B, except that the indicated solutes were present in both solutions prior to mixing. Fits shown are to a single exponential decay (eq. 3), with parameters listed in Table 3.

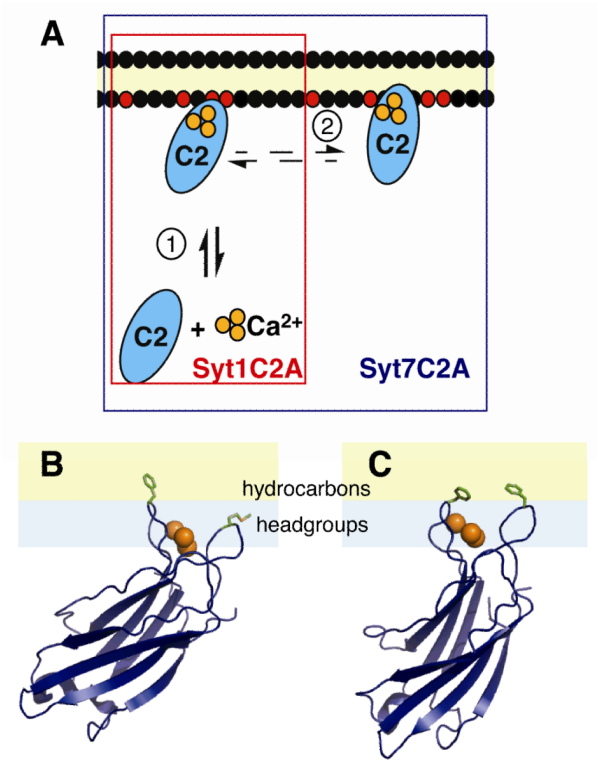

Figure 6. Model of Syt7 C2A membrane docking mechanism

A: Proposed two-step docking model. In step 1, C2 domains interact with Ca^{2+} ions (orange circles) to drive initial electrostatic docking to membranes containing anionic lipid headgroups (red circles). Both Syt1 C2A (red box) and Syt7 C2A (blue box, inclusive of both steps) can participate in this docking event. In this model, Syt7 C2A but not Syt1 C2A can also undergo a transition to a more deeply inserted docking geometry (step 2). **B:** Membrane docking geometry for Syt1 C2A previously determined through electron paramagnetic resonance (EPR) depth measurements (13). The published solution structure of Ca^{2+}-bound Syt1 C2A (PDB ID 1BYN (62)) is drawn aligned to the membrane in an illustration of the EPR-determined geometry reported by Frazier, *et al.* (13). The amino acid sidechains of Phe234 and Met173 on the membrane-inserted Ca^{2+} binding loops are shown (green sticks). **C:** Hypothesized membrane docking geometry of Syt7 C2A. The solution structure of Syt7 C2A (PDB ID 2D8K) is drawn aligned to the membrane in a manner allowing penetration of both Phe229 and Phe167 (green sticks) into the hydrocarbon interior of the membrane. For clarity in illustration, three Ca^{2+} ions were modeled into the Ca^{2+}-free 2D8K structure based on their position in 1BYN after backbone alignment of the two structures. Panels B and C were created using MacPyMol.

Table 1

Physiological target membrane lipid compositions (%)

Membrane	PC	PS	PE	PI	PG	CH	SM	PIP_2	dansylPE
TM(−)PIP_2	10.7	21.3	27.9	5.6	0	25	4.5	0	5
TM(+)PIP_2	10.7	21.3	27.9	4.6	0	25	4.5	1	5
TM[11%PS]	10.7	11.3	37.9	5.6	0	25	4.5	0	5
TM[31%PS]	10.7	31.3	17.9	5.6	0	25	4.5	0	5
TM(−)PS/PI(+)PG	10.7	0	27.9	0	26.9	25	4.5	0	5

Table 2

Best-fit parameters from equilibrium calcium titrations

Protein domain	Membrane	$Ca_{1/2}$ (μM)[a]	Hill coefficient[a]
Syt1 C2A	1:1 PC:PS/5%dPE	31 ± 2	2.4 ± 0.4
Syt1 C2A	TM(−)PIP_2	43 ± 1	1.8 ± 0.1
Syt1 C2A	TM(+)PIP_2	37 ± 1	1.9 ± 0.1
Syt7 C2A	1:1 PC:PS/5%dPE	1.7 ± 0.2[b]	2.2 ± 0.1
Syt7 C2A	TM[11%PS]	8 ± 1[b]	2.6 ± 0.1
Syt7 C2A	TM(−)PIP_2	5.4 ± 0.4[b]	2.7 ± 0.2
		4.7 ± 0.2	3.4 ± 0.5
Syt7 C2A	TM[31%PS]	2.2 ± 0.1[b]	2.0 ± 0.1
Syt7 C2A	TM(+)PIP_2	3.4 ± 0.2	2.8 ± 0.4
Syt7 C2A	TM(−)PS/PI(+)PG	5.1 ± 0.3[b]	3.0 ± 0.1
PKCα C2	TM(−)PIP_2	30 ± 10	1.0 ± 0.1
PKCα C2	TM(+)PIP_2	7.7 ± 0.5	1.9 ± 0.1

[a]Best-fit parameters were determined by fitting titration data to the Hill equation (Eq. 1). The mean and standard deviation of these parameters are reported from at least three independent titrations for each protein-membrane pair.

[b]Titration performed in a Ca^{2+} buffering system using NTA (see Methods).

Table 3

Measured rate constants from kinetic experiments

Protein domain	k_{off} (s^{-1})[a]	k_{obs} for association (s^{-1})	k_{off}/k_{on} (μM)[b]
Syt1 C2A	670 ± 20[c]	340 ± 10	41 ± 2
Syt7 C2A	11 ± 4	157 ± 2	1.5 ± 0.5
PKCα C2	50 ± 2	64 ± 2	16 ± 1
$cPLA_2$ C2	15 ± 1	37 ± 2	N.D. [d]
Syt1 C2A (30% trehalose)	660 ± 10	N.D.	N.D.
Syt7 C2A (30% trehalose)	4.5 ± 0.5	N.D.	N.D.
Syt7 C2A (1.3 M Na_2SO_4)	2.0 ± 0.1	N.D.	N.D.
Syt7 C2A (1.3 M NaCl)	40 ± 3	N.D.	N.D.

[a] Values and errors shown are from best-fits to representative data averaged over 8-12 repeat measurements for each condition. All experiments used TM(−)PIP2 membranes.

[b] Values of k_{on} were determined by dividing k_{obs} by the concentration of accessible PS (see Discussion).

[c] Dissociation kinetics for Syt1 C2A were biexponential. The major rate (90% of amplitude) is reported.

[d] N.D.: Not determined. Because $cPLA_2$ C2 interacts with PC rather than PS, k_{off}/k_{on} is not reported for this domain.

Table 4

Single-molecule diffusion measurements

	Diffusion constant of fluorescent species ($\mu m^2/s$) [a]		
Unlabeled Syt7 C2A added	AF647-Syt7C2A	AF555-PKCαC2	AF555-cPLA$_2$C2
0 nM	1.5 ± 0.1	1.6 ± 0.1	1.5 ± 0.1
20 nM	1.3 ± 0.1	1.5 ± 0.1	N.D.
60 nM	0.8 ± 0.2	1.0 ± 0.1	0.9 ± 0.1

[a] Values and errors shown are mean ± S.D. from 3-6 movies of 1000 frames each, and are obtained by fitting diffusion data pooled from all trajectories of each movie (600-6000 steps per movie). Measurements were taken on DOPC:DOPS (3:1) membranes at 200 μM Ca^{2+}. N.D.: Not determined.